IEEE Access
Multidisciplinary | Rapid Review | Open Access Journal

Received March 24, 2020, accepted April 15, 2020, date of publication April 24, 2020, date of current version May 11, 2020.

Digital Object Identifier 10.1109/ACCESS.2020.2990131

Changing the Operation of Small Geometrically Complex EBG-Based Antennas With Micron-Sized Particles That Respond to Magneto-Static Fields

ADNAN IFTIKHAR[1], (Member, IEEE), SAJID MEHMOOD ASIF[2], (Member, IEEE), JACOB M. PARROW[3], JEFFERY W. ALLEN[4], (Senior Member, IEEE), MONICA S. ALLEN[4], (Senior Member, IEEE), ADNAN FIDA[1], and BENJAMIN D. BRAATEN[3], (Senior Member, IEEE)

[1]Electrical and Computer Engineering, COMSATS University, Islamabad 44000, Pakistan
[2]Electronic and Electrical Engineering, The University of Sheffield, Sheffield S1 4ET, U.K.
[3]Department of Electrical and Computer Engineering, North Dakota State University, Fargo, ND 58102, USA
[4]AFRL/RWMFT Air Force Research Laboratory, Munitions Directorate, Valparaiso, FL 32542, USA

Corresponding authors: Adnan Iftikhar (adnaniftikhar@comsats.edu.pk) and Benjamin D. Braaten (benbraaten@ieee.org)

This work was supported by the US Air Force Research Laboratory Munitions Directorate under Grant FA-8651-15-2-002.

ABSTRACT As the usage of wireless technology grows, there are evermore demands on the antennas that support these platforms. This need has led to the design of unique antennas with improved bandwidth, agile frequency capabilities, compact size and greater efficiencies. In part though, the trade-off for such capabilities is antenna complexity. This paper presents a new technique for simplifying the method of changing the operation of a printed antenna using micron-sized silver coated particles that respond to magneto-static fields. More specifically, a structure consisting of a low-loss dielectric material with a cylindrical cavity containing micro-sized particles is developed. The overall size of the dielectric material is 1.5 mm$\times$1.5 mm$\times$0.5 mm and the cavity has a diameter of 0.9 mm. Furthermore, the top and bottom of the cavity with the micron-sized particles is capped with copper foil. Then, to manipulate the enclosed particles, a static magnet is placed near the structure. The enclosed particles columnize and orientate in the direction of the field-lines, connecting the top and bottom copper foil plates. To disconnect the plates then, the field is simply removed and the columns collapse. Macroscopically, the structure has the behavior of a switch. The structures presented in this work are denoted as Magneto-static Field Responsive Structures (MRSs). The MRSs have an additional benefit of not requiring a direct connection to a biasing circuit. This is very useful because there are many antenna designs that make it difficult to embed biasing circuitry to reconfigure printed antennas using MEMS and PIN diodes, for example. Finally, a new frequency reconfigurable Electromagnetic Band Gap (EBG) antenna is presented. This design is unique because the complex layout does not allow for traditional biasing circuitry and the operation is changed using the new MRSs presented in this paper.

INDEX TERMS EBG structures, magneto-static responsive structures (MRSs), printed antennas, reconfigurable antennas.

I. INTRODUCTION

Antennas with features such as compact geometries, unique frequency agile characteristics and ease of use continue to be of great interest to antenna researchers and designers in many different areas [1]–[3]. Creating compact antennas with frequency agile characteristics are of particular interest in areas such as wireless sensors, aerospace systems and portable multi-radio platforms (i.e., mobile internet devices, laptops, smart phones etc.). These systems are being required to access multiple wireless services such as WiFi, WiMax, 3G, Bluetooth, GPS and UWB over various frequency bands [4].

Reconfigurable antennas is an area where there has been significant development on using various methods for controlling the agility of antennas. These efforts have shown promising results that most commonly include using Field Effect Transistors (FETs), PIN diodes and MEMS devices to enable frequency reconfigurable antennas [5]–[12].

The associate editor coordinating the review of this manuscript and approving it for publication was Giorgio Montisci.

Other methods such as liquid metals [13], stepper motors [14], reed switches [15]–[17], optical circuitry [18], and fluidic micro-pumps [19] have also been demonstrated as additional methods to control the frequency characteristics of antennas. However, with the exception of the designs reported in [15]–[17], these techniques require a direct connection with biasing circuitry. This can be a drawback because the circuitry could have a negative impact on the pattern of the antenna because of the component placement near radiating elements [20] and a complex geometry may make it very difficult to embed this circuitry into the design.

Furthermore, hardware limitations of modern wireless systems require electrically small antennas and it is becoming more challenging to achieve several bands using a single antenna without compromising on efficiency and radiation characteristics. Miniaturized microstrip patch antennas owing to their simple structure, compact footprint, and ease of integration have been considered prime candidates for wireless communication systems as compared to printed monopoles and dipole antennas. Miniaturization of the microstrip patch antennas have been achieved using slots, defected ground planes, and loading with metamaterials [21]. The loading of patch antennas with metamaterials such as EBGs or High Impedance Surfaces (HIS) significantly reduce antenna size and result in a complex structure that may be difficult to reconfigure using existing RF switches because of embedment of the directly connected biasing circuitry [22]. Therefore, the objective of this paper is to implement a new component, shown in Figure 1 (a), that does not require a directly connected biasing circuit for reconfiguring the complex EBG inspired antenna design in Figure 1 (b). Because of the compactness and complexity of the antenna in Figure 1 (b), reconfigurability could not be easily achieved with conventional methods (PIN diodes and MEMS) that use directly connected biasing lines and was convenient with the structures in Figure 1 (a).

The results reported in [15]–[17], [20] are among the first designs that do not require a direct connection with biasing circuitry to reconfigure the antenna. Some of these were achieved using a reed switch [23]. Overall, the results were very promising and showed that a printed antenna could be successfully developed; however, due to the size of the reed switches it may be difficult to implement several of these into the design of an electrically small antenna. Furthermore, because of the geometry of the switches, embedding them into the substrate of an antenna is both challenging and impractical. The structure presented in Figure 1 (a) is a new approach to overcome these potential design obstacles.

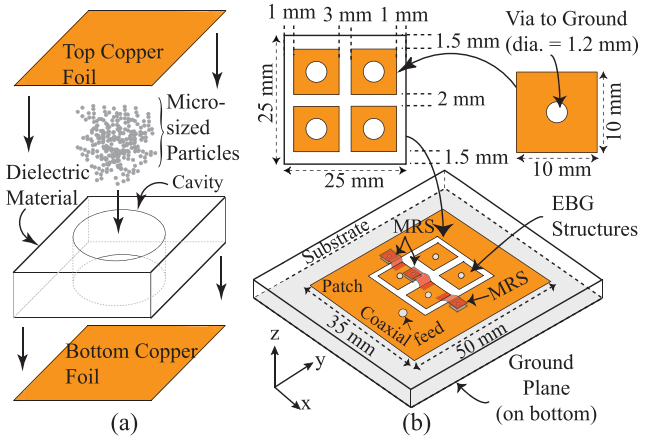

FIGURE 1. (a) Expanded view of the Magneto-static Field Responsive Structures (MRSs) and (b) Drawing of the small geometrically complex antenna reconfigured using the MRSs.

II. THE MAGNETO-STATIC FIELD RESPONSIVE STRUCTURES

A. BEHAVIOR OF THE STRUCTURES

The proposed structure (i.e., component) shown in Figure 1 (a), consists of a low loss dielectric material with a cylindrical cavity. The cylindrical cavity was partially filled with silver coated micro-sized particles using a technique reported in [24] that contained a core that responded to magneto-static fields. To enclose the cavity, the top and bottom layers of the dielectric material were covered (i.e., capped) with a copper foil. Then, when a static magnetic field was applied to the structure, the particles formed columns in the direction of the field lines, as shown in Figure 2. Since the particles were coated in silver, this created a conducting path between the top and bottom copper plates. Next, when the field was removed, the columns disassembled, as shown in Figure 2, and the two plates were disconnected. This resulted in a behavior similar to a switch. The structures presented in Figures 1 (a) and 2 are denoted as Magneto-static Field Responsive Structures (MRSs) [20]. Since the field-lines control the particles in the cavity, the MRSs have an additional benefit of not requiring a direct connection to a biasing circuit. Again, this makes them particularly suitable for embedding into complex antenna geometries, compact design layouts, and potentially dielectric substrates/superstrates.

B. RESPONSE OF THE PARTICLES TO THE MAGNETO-STATIC FIELD

The silver coated particles used throughout this paper were manufactured by Potters Industries [25] (CONDUCT-O-Fil,

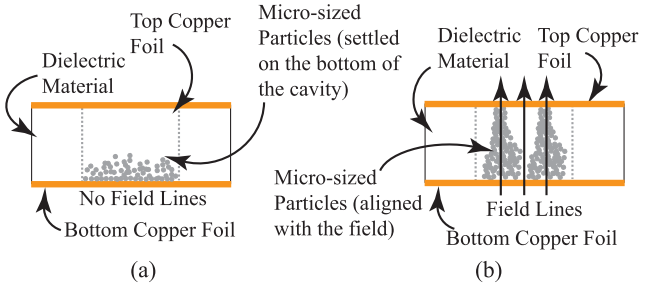

FIGURE 2. (a) Side-view of the MRSs in the absence of a magneto-static field showing the particles on the bottom of the cylindrical cavity and (b) Side-view of the MRSs in the presence of a magneto-static field showing the particles aligning with the field lines.

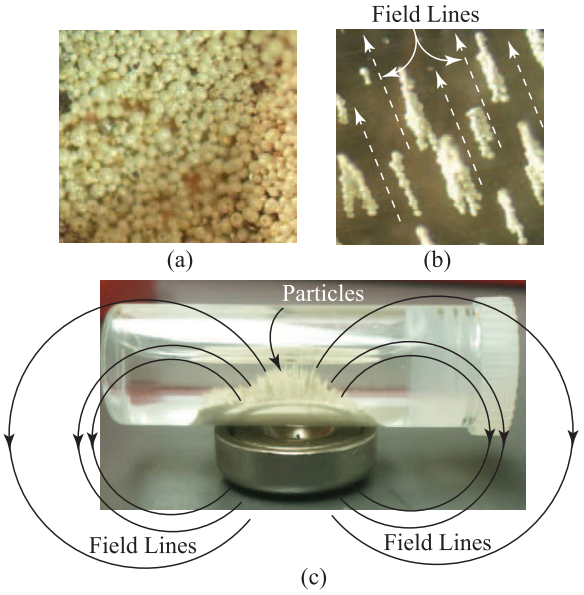

FIGURE 3. (a) Photograph of the particles under a microscope; (b) photograph of the particles columnizing on a flat surface in the direction of the field-lines; and (c) photograph of the particles initially dissolved in alcohol aligning with the field lines.

part number SM40P20). A picture of the particles (under a microscope) is shown in Figure 3 (a) and diameter of the particles are between 10 - 40 microns. To demonstrate the response of the particles in the presence of a magneto-static field, a sample was placed above a permanent magnets (as shown in Figure 3 (c)). The particles then columnized in the direction of the field lines and this phenomena is shown in Figure 3 (b) and (c). This is the mechanism used to change the states of the MRSs in Figure 1 (a). This is because with a sufficient amount of particles in a cavity, these columns are used to electrically connect the two copper foil plates.

C. MANUFACTURING OF THE MAGNETO-STATIC RESPONSIVE STRUCTURES

The next step was to determine the amount of particles required to manufacture and successfully control various MRSs. Several different geometries were manufactured and tested. The two dimensions of particular interest for this paper are shown in Figures 4 and 5. The dielectric material chosen was TMM4, which was manufactured by Rogers Corporation [26]. These dimensions were chosen because: (1) prototypes could be conveniently manufactured using standard PCB milling machine practices [24]; (2) the cavities could be filled under a microscope using repeatable techniques; and (3) the overall size of the manufactured prototypes were small enough for embedding into the proposed antenna, shown in Figure 1 (b). For the quantification of magnetic particles, a measuring cup having a cylindrical cavity with 0.2 mm radius and thickness (h) of 0.254 mm was manufactured, as shown in Figure 6. The amount of particles (N) that filled the manufactured cylindrical cavity was first estimated

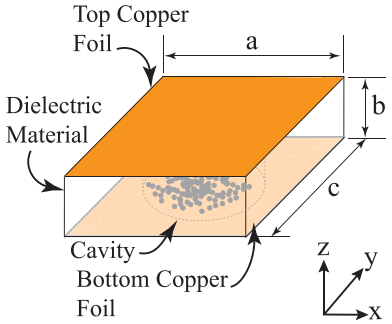

FIGURE 4. Geometry of the prototype MRSs.

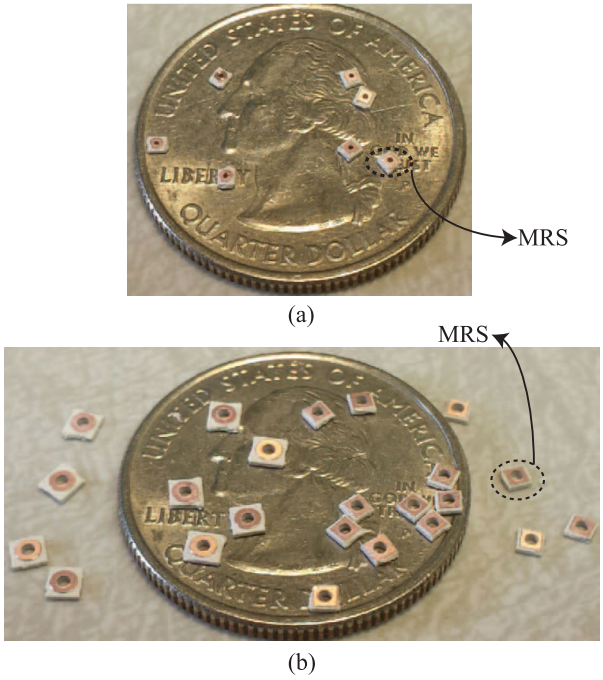

FIGURE 5. Photographs of the manufactured MRS cavities with (referring to dimensions shown in Figure 4) (a) $a = 1.0$ mm, $b = 0.508$ mm, $c = 1.0$ mm and a cavity diameter of 0.4 mm and (b) $a = 1.5$ mm, $b = 0.508$ mm, $c = 1.5$ mm and a cavity diameter of 0.9 mm.

mathematically, as [27]

$$N = \left(\frac{\pi}{3\sqrt{2}}\right)\left(\frac{\pi r^2 h}{4/3\pi R^3}\right). \quad (1)$$

The term $\frac{\pi}{3\sqrt{2}}$ in equation (1) is the densest possible arrangement of spherical particles in a three-dimensional cylindrical enclosure and is defined by Kepler's formula [27]. Also, in equation (1), the numerator term is the volume of the cylindrical cavity and the denominator is the volume of spherical magnetic particles with an average diameter of 40 μm. Further simplification of equation (1) is given in equation (2):

$$N = \frac{\pi r^2 h}{4\sqrt{2}R^3} \cong 704, \quad (2)$$

where, r is the radius of the cylindrical cavity drilled in the measuring cup, h is the height of the cylindrical cavity, and R is the average radius of the spherical magnetic particle, i.e 20 μm. Substituting values in equation (2) showed that

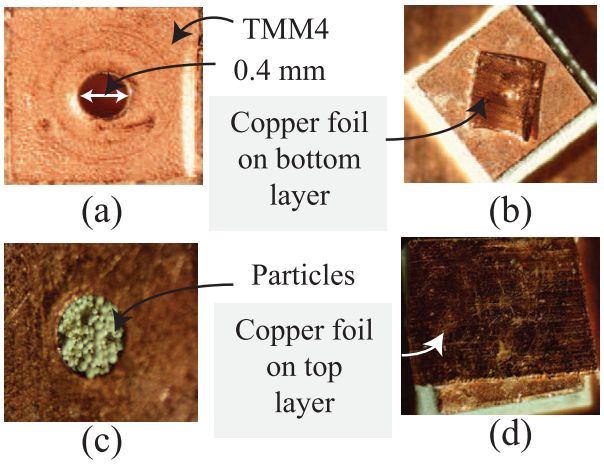

FIGURE 6. Experimental verification of the magnetic particles in a cavity: (a) picture of manufactured measuring cup, (b) copper sheet on the bottom side of cavity to avoid sticking of the magnetic particles with the copper tape, (c) measuring cup filled with the magnetic particles, and (d) copper tape on the bottom side.

the measuring cup shown in Figure 6 can hold a maximum of 704 magnetic particles.

For the analytical verification of quantification of particles, a measuring cup was completely filled with the magnetic particles, as depicted in Figure 6 (a) - (d)). These filled particles were then transferred from the measuring cup cavity to a flat piece of sheet using a small magnet under the measuring cup. The flat sheet was placed under a microscope and magnetic particles were counted. This procedure was performed five times and counted particles were found to be 700, 708, 702, 703 and 704 for five experiments, respectively. It was therefore concluded that a measuring cup of 0.2 mm radius and 0.254 height, shown in Figure 6 could hold an average of 704 particles, approximately.

Following the analytical and experimental quantification of magnetic particles, the measuring cup procedure was adopted to fill the cavity of MRSs. A small hole of 0.1 mm radius (less than that of MRS radius) was drilled in a material sheet where particles were transferred from the measuring cup. Next, the hole of the sheet was placed on the top of the Magneto-static Responsive Structure (MRS) cavity and a small permanent magnet was used to move particles into the host cavity. A complete procedure of filling the magnetic particles in the MRS cavity is depicted in Figure 6. It was therefore concluded that to fill the MRS cavity with sufficient number of magnetic particles to form columns in the presence of a magnetic field, a small measuring cup with cavity height less than the MRS cavity height was first fully filled with magnetic particles, as explained in Figure 6 (a)-(d). Then, the magnetic particles in the measuring cup were migrated to a sheet of paper to fill the host MRS cavity having a larger thickness (height) as compared to the measuring cup, as shown in Figure 7. The minimum magnetic field strength to columnize the particles was 300-350 Gauss for the embodiments shown in Figure 5.

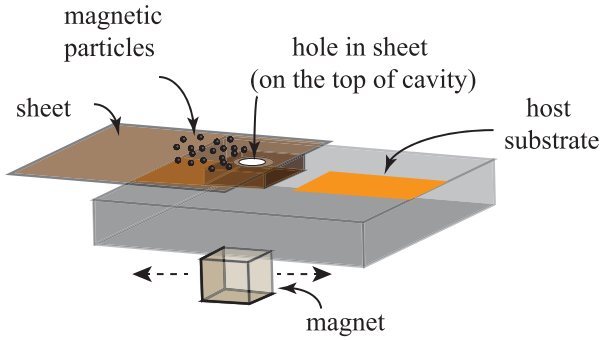

FIGURE 7. Method used to migrate particles into the MRS cavity.

III. MODELING THE MAGNETO-STATIC RESPONSIVE STRUCTURES

The Magneto-static Responsive Structures (MRSs) cavities shown in Figure 5 were modeled in the 3D simulation software ANSYS High Frequency Simulation Software (HFSS) [28] to observe their RF behavior in the absence and presence of a magnetic field. A 50 Ω transmission line (TL) with a gap of 0.3 mm was designed in HFSS on the Rogers TMM4 1.524 mm thick substrate. Then, 1.5 mm x 1.5 mm MRSs with a 0.508 mm height having a 0.9 mm cavity diameter was modeled in HFSS. The bottom side of Magneto-static Responsive Structure (MRS) was placed on the one side of the discontinuous TL, whereas the top side of the MRS cavity was connected to the other discontinuous TL using a copper sheet. Figure 8 shows the complete geometry of the MRS and TL modeled in the simulation software. In simulations, to mimic the MRS 'OFF' state and the absence of the magnetic field, silver coated spheres were placed on the bottom of the MRS cavity. On the other hand, 25 columns of spherical shaped magnetic particles, as shown in Figure 8 (b), were modeled in the simulation with an average diameter of 40 μm which provided a connection between the bottom and copper tape of the MRS. A parametric study was also performed on the number of columns of modeled magnetic particle spheres to analyze the S-parameter variation and optimize the simulation time. The $|S_{11}|$ (dB) results for the 1, 2, 4, and 25 columns are shown in Figure 9. It was observed that the number of columns do not effect the $|S_{11}|$ (dB) and $|S_{22}|$ (dB) values over the entire frequency range. It was also observed that 25 consumed more simulation time as compared 1 column.

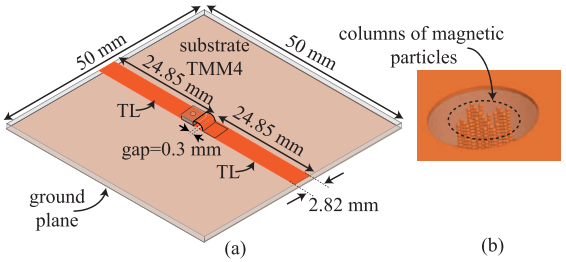

FIGURE 8. (a) Dimensions of a 50 Ω TL with the MRS modeled in HFSS and (b) magnetic particles modeled as conducting spheres and columns of magnetic particles to show MRS 'ON' state.

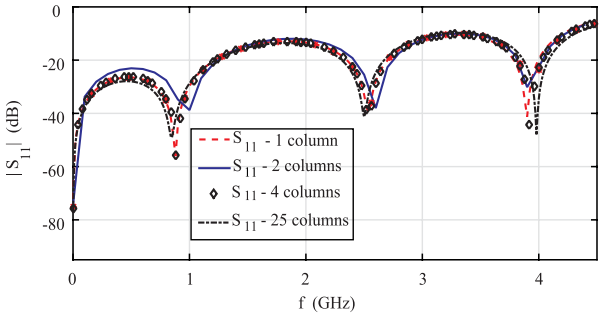

FIGURE 9. A comparison of the simulated $|S_{11}|$ (dB) values for a various number of columns of magnetic particles in the MRS cavity.

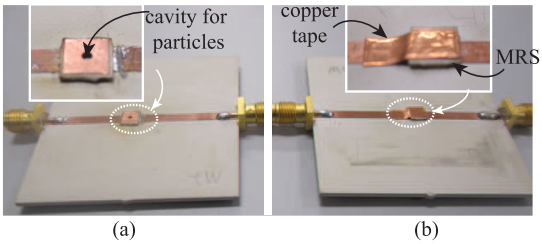

FIGURE 10. (a) A Photograph of the prototype MRS attached to 50 Ω TL and (b) a photograph of the prototype MRS on host TL with magnetic particles and connected with copper tape.

Therefore, one column was used in simulations to model the MRS 'ON' state and to save computational time.

Moreover, the TL having the same dimensions as given in Figure 8 was fabricated, and the manufactured MRS was then attached to the host discontinuous TL. A picture of the fabricated prototype with the MRS is shown in Figure 10.

Figure 11 shows the S-parameters of the MRS on a TL in a magnetically 'unbiased' state. It can be observed from Figure 11 that when there is an absence of the magnetic field, the magnetic particles in the MRS cavity did not columnize themselves and a mismatch existed at the TL ports and better isolation of 15 dB up-to 4.5 GHz was obtained. However, when the external magnetic field was applied, the magnetic particles aligned in columns and provided a continuous path for the propagation of the electromagnetic (EM) wave with good impedance matching characteristics at the ports, as depicted in Figure 12. It can also be observed from Figure 12 that EM wave is propagating in the presence of static magnetic field ($|S_{21}|$ magnitude is around 0.7 dB-0.85 dB at low frequencies and goes up to 1.5 dB at higher frequencies). Therefore, it was concluded that the MRS on a discontinued TL acts as a radio frequency (RF) switch in the presence and absence of the applied magnetic field and have switching capabilities from 100 KHz to 4.5 GHz. Overall, a good agreement was observed in the simulation and measurement results.

IV. EMBEDDING THE MAGNETO-STATIC RESPONSIVE STRUCTURES INTO AN EBG ANTENNA

The demonstration of the proposed MRSs as an RF switch showed that these MRSs could be used in achieving

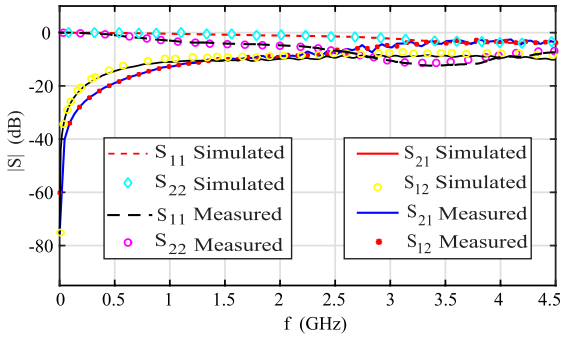

FIGURE 11. S-parameter comparison of measurement and simulation results of the MRS embedded on a discontinuous TL in the absence of the magnetic field.

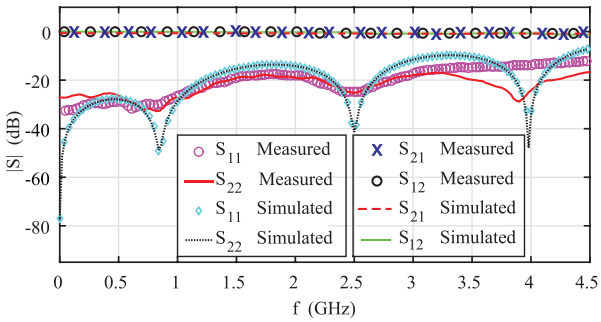

FIGURE 12. S-parameter comparison of the measurement and simulation results of the MRS embedded on a discontinuous TL in the presence of the magnetic field.

frequency agility and has potential to have benefits over the conventional switches such as PIN diodes and MEMS etc. Also, the proposed MRSs do not require biasing circuitry for their operation as compared to conventional solid-state RF switches and have an additional embedding feature on the host substrate. Therefore, to further highlight the application of the proposed MRSs, a complex EBG antenna shown in Figure 1 (b) that was difficult to frequency reconfigure using the existing RF switching technologies was designed and the proposed MRSs were used to achieve frequency agility.

V. EBG ANTENNA GEOMETRY, PROTOTYPING AND MRSs INTEGRATION

The layout of the proposed antenna is shown in Figure 1. The proposed design is probe fed having partially filled with 2 x 2 mushroom like EBG structures in a rectangular patch antenna. The selected substrate was a low loss RT/duriod 5880 from Rogers Corporation, with a 0.254 thickness (H), 2.2 permittivity (ϵ_r), and a loss tangent $\tan\delta = 0.0009$. The proposed antenna resonated at a lower frequency if a current path was provided between the patch to EBG 1, EBG 1 to EBG 2, and then EBG 2 to patch. On the other hand, the antenna resonated at a higher frequency when the current concentration was isolated between the EBG structures and rectangular patch antenna. To control these currents then, frequency reconfigurability of the EBG antenna is proposed. Unfortunately, DC biasing circuitry could not be incorporated

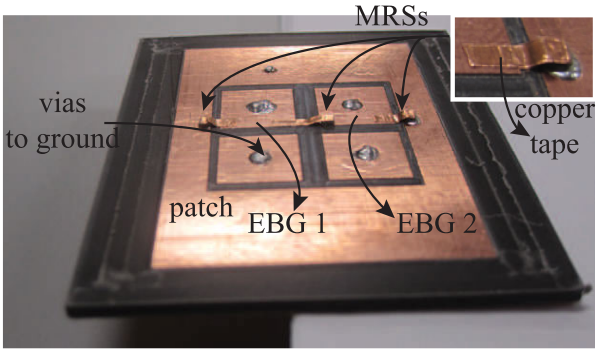

FIGURE 13. Photograph of the fabricated EBG antenna with the MRSs (with magnetic particles and copper tape).

in the proposed configuration because of the polarity issues and ground plane connection of the vias in the EBG structures. Therefore, the proposed design configuration was not possible to reconfigure using existing RF switching devices and this shows the limitation of the existing devices (like PIN diodes) and highlights the application of the proposed MRSs.

The proposed EBG antenna was reconfigured by embedding three MRSs. The three MRSs were modeled with the EBG antenna having the dimensions shown in Figure 1 in the full-wave EM software, HFSS [28]. To experimentally validate the design concept and embedding of the MRSs for frequency reconfigurability, the EBG antenna was fabricated and MRSs were manufactured. The manufactured MRSs were attached to the fabricated antenna and the cavities were partially filled with the magnetic particles using the measuring cup method. A photograph of the fabricated prototype with the MRSs attached to the EBG antenna is shown in Figure 13. A small permanent magnet under the EBG antenna with MRSs attached was used to produce static magnetic field for the columnization of particles in the cavity. In the absence of an external magnetic field, the magnetic particles in the MRS cavities settled down and provided RF current isolation between the EBG structures and rectangular patch. This resulted in smaller dimensions of the EBG antenna and resonance at a higher frequency, i.e., 2.21 GHz. On the other hand, when an external field was applied, magnetic particles in the cavities columnized themselves and provided a current path between the patch to EBG 1, EBG 1 to EBG 2, and then EBG 2 to patch. Therefore, the overall electrical length increased and the EBG antenna resonated at 930 MHz.

VI. RESULTS AND DISCUSSION

The current distribution of the EBG antenna embedded with MRSs was also analyzed and is presented in Figure 14. It can be observed from Figure 14 that the current distribution detours around the slots between the EBG structures and the rectangular radiating portion in the absence of an external magnetic field. So, current was mainly distributed on the patch, this made the electrical length of the antenna shorter and the EBG antenna resonated at a higher frequency in the MRSs 'OFF' state (absence of magnetic field).

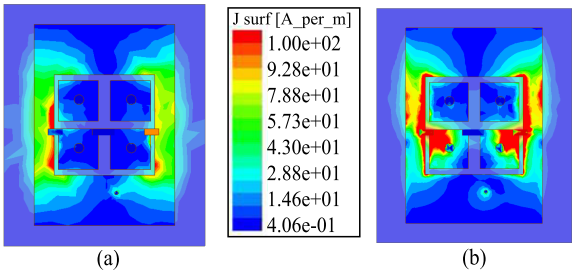

FIGURE 14. Surface current distribution: (a) MRSs 'OFF' state and (b) MRSs 'ON' state.

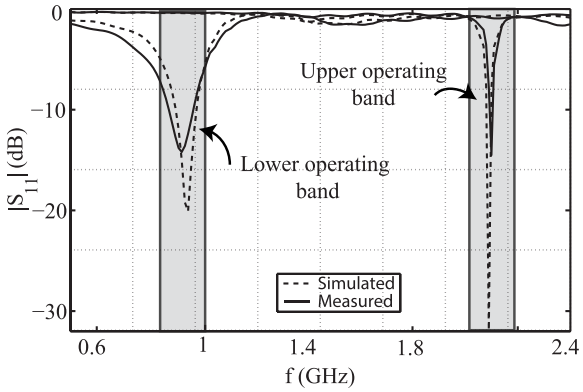

FIGURE 15. Simulated and measured S-parameter of the EBG antenna embedded with novel MRSs.

However, in the presence of the magnetic field, current passed through the MRSs and concentrated in both the EBG and patch, as depicted in Figure 14 (b). This increased the electrical length of the EBG antenna and showed resonance at 930 MHz.

The MRSs were used to achieve two useful states; 'OFF' and 'ON' for achieving frequency reconfigurability in the design which was difficult to reconfigure using existing RF switching techniques. HFSS was used for the simulation of the EBG antenna and MRSs, whereas a calibrated Agilent E5071C Vector Network Analyzer (VNA) was used for the measurements of the S-parameters. Figure 16 shows the simulated and measured S-parameters of the frequency re-configured EBG antenna using the proposed MRSs.

Furthermore, the normalized Gain theta (G_θ) and Gain Phi (G_ϕ) components of the radiation patterns in the E-plane (and H-plane) of the EBG antenna embedded with MRSs were also analyzed and measured in a fully calibrated anechoic chamber to observe the effect of the static magnetic field due to the permanent magnet on the far-field characteristics. A picture of the prototype taken during the radiation pattern measurements is depicted in Figure 16. The simulated and measured results are presented in Figure 17. At both switching frequencies, broadside radiation patterns are obtained. The G_θ and G_ϕ components of E- and H-plane showed that polarization of the antenna remained the same during the reconfigurability operation using the proposed MRSs. A good agreement between the simulation and measurement results confirmed that use of the external magnet on the bottom side

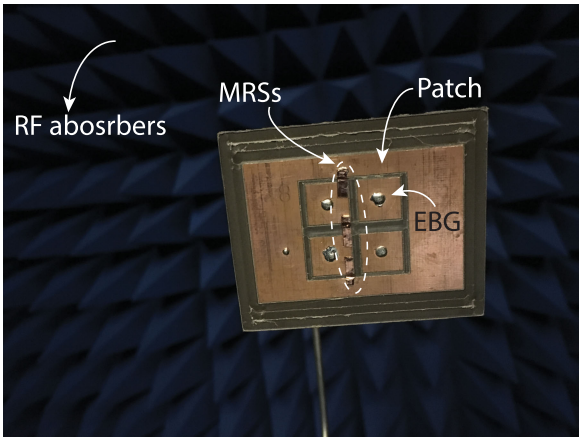

FIGURE 16. A picture of the prototype taken during the radiation pattern measurements in a fully calibrated anechoic chamber.

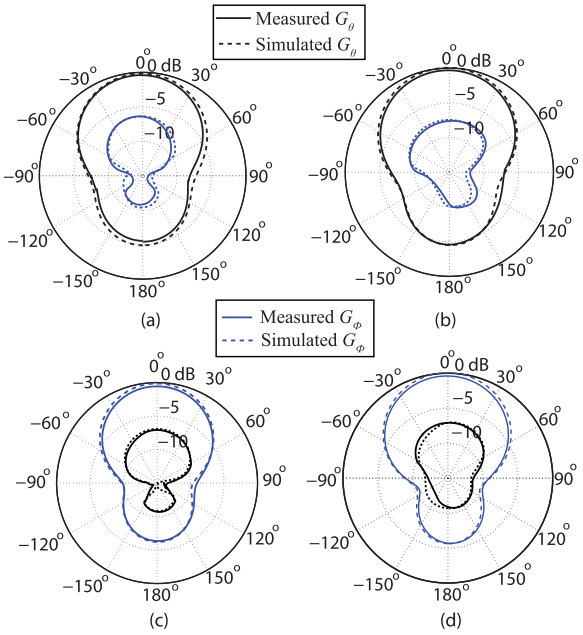

FIGURE 17. Simulated and measured normalized radiation patterns in the (a) E-plane (Gain theta (G_θ) and Gain Phi (G_ϕ) components) when magnetic field is absent for MRSs, (b) E-plane (G_θ and G_ϕ components) when external magnetic field is present for MRSs, (c) H-plane (G_θ and G_ϕ components) when magnetic field is absent for MRSs, and (d) H-plane (G_θ and G_ϕ components) when external magnetic field is present for MRSs.

of EBG antenna did not affect the far-field performance of the sample antenna. The gain of the antenna in the presence and absence of the external static magnetic field to switch 'ON' and 'OFF' was also measured. At 2.21 GHz the measured gain of the EBG antenna was 5.26 dBi, whereas, 3.8 dBi gain was obtained at 930 MHz. It was also observed that the embedded MRSs did not degrade the antenna radiation performance and instead improved the gain and efficiency as reported in [20] because these structures did not require biasing circuitry for their operation.

Conventional devices such as PIN diodes, FETs, and MEMS switches for reconfigurable operation offer reliable switching speeds, dynamic reconfiguration, and ease of packaging. PIN diodes usually offer switching speeds ranging from 1-100 nsec [29] and have high power handling capability. Whereas, MEMS have switching speeds from 1-200 μsec which are considered low for practical reconfiguration operations [30]. MEMS may be considered superior to PIN diodes and FETs, as they have low loss and a high Quality (Q) factor. Despite of the mentioned advantages of microelectromechanical (MEMS) and active switches (PIN diodes or FETs), the requirement of DC biasing circuitry is still present and in some cases these devices degrade the power efficiency and antenna performance [20]. For instance, performance degradation analysis of reconfigurable slot ring antenna using PIN diodes in [31] showed that the gain drops from 5.72 dB to 5.2 dB at 7.26 GHz when switches are used. Similarly, a comparison on the radiation performance of reconfigurable microstrip patch antenna using PIN diodes and proposed MRS in [20] reveal that PIN diodes degrade the antenna gain to 2.3 dBi in the 'ON' state as compared to the proposed MRS (4 dBi in MRS 'ON' state). Furthermore, a geometrically complex antenna can make it very difficult (or make impossible) to use biasing circuitry in the design without significantly affecting the antenna performance.

This paper presented novel MRSs that do not require any metallic vias, chip inductors, and dc bias lines as required by FETs, PIN diodes, and MEMS. Followed by the working principle and performance of the proposed novel structures as a RF switch on a discontinuous TL, the advantage of MRSs was demonstrated by designing a sample antenna that was hard to reconfigure using existing RF switching technologies. Simulated and measured results verified that use of static field to activate the proposed MRSs did not degrade return loss and far-field performance of the stand-alone antenna system and can frequency reconfigure the antenna. The switching characteristics of the proposed MRS on a discontinuous TL showed that proposed switch has an insertions loss ($|S_{12}|$ (dB)) ranging from 0.7-0.85 dB at a frequency range from 100 KHz to 3.5 GHz. Whereas, the insertion loss increases to 1.5 dB over the frequency range from 3.5 GHz to 4.5 GHz. This limitation of high insertion loss in the prototype MRS as compared to PIN diodes and MEMS can be overcome by proper packaging of the proposed MRS. In addition, the use of a permanent magnet to provide a static magnetic field for the switching of MRSs may not be useful for all applications. Therefore, the use of a control circuit using photoelectric couplers for the reed switches [32] could possibly be used to provide a static magnetic field for the activation of the MRSs. Another practical method to apply a static magnetic field to activate MRS can be use of copper/silver coil around the particle cavities [15]. Furthermore, research on activating the proposed MRSs here is still needed.

VII. CONCLUSION

In this paper, a rectangular structure consisting of low loss dielectric material having an overall size of 1.5 mm x 1.5 mm with a cavity diameter of 0.9 mm containing micron-sized magnetic particles was developed. The proposed novel

Magneto-static Responsive structures (MRSs) working as a RF switch from 100 KHz to 4.5 GHz was demonstrated along with the quantification of the magnetic particles in the MRS cavity. It was shown successfully that the proposed MRSs have a compact size and can be embedded on printed antennas to achieve agile frequency capabilities. Furthermore, this work demonstrated the potential of the MRS by employing it to achieve frequency agility of a complex EBG antenna, which could not otherwise be achieved using either PIN diodes or MEMS. The new MRSs were embedded on the complex EBG antenna layout and the operating frequency was changed from 2.21 GHz to 900 MHz using MRSs. Overall, good agreement was observed between simulation and measurement results.

REFERENCES

[1] M.-C. Tang and R. W. Ziolkowski, "Frequency-agile, efficient, circularly polarized, near-field resonant antenna: Designs and measurements," *IEEE Trans. Antennas Propag.*, vol. 63, no. 11, pp. 5203–5209, Nov. 2015.

[2] N. Nguyen-Trong, T. Kaufmann, L. Hall, and C. Fumeaux, "Analysis and design of a reconfigurable antenna based on half-mode substrate-integrated cavity," *IEEE Trans. Antennas Propag.*, vol. 63, no. 8, pp. 3345–3353, Aug. 2015.

[3] D. Wu, S. W. Cheung, and T. I. Yuk, "A compact and low-profile loop antenna with multiband operation for ultra-thin smartphones," *IEEE Trans. Antennas Propag.*, vol. 63, no. 6, pp. 2745–2750, Jun. 2015.

[4] S. Yang, C. Zhang, H. K. Pan, A. E. Fathy, and V. K. Nair, "Frequency-reconfigurable antennas for multiradio wireless platforms," *IEEE Microw. Mag.*, vol. 10, no. 1, pp. 66–83, Feb. 2009.

[5] L. N. Pringle, P. H. Harms, S. P. Blalock, G. N. Kiesel, E. J. Kuster, P. G. Friederich, R. J. Prado, J. M. Morris, and G. S. Smith, "A reconfigurable aperture antenna based on switched links between electrically small metallic patches," *IEEE Trans. Antennas Propag.*, vol. 52, no. 6, pp. 1434–1445, Jun. 2004.

[6] P. Lu, K. M. Huang, Y. Yang, F. Cheng, and L. Wu, "Frequency-reconfigurable rectenna with an adaptive matching stub for microwave power transmission," *IEEE Antennas Wireless Propag. Lett.*, vol. 18, no. 5, pp. 956–960, May 2019.

[7] H. Song, S.-H. Oh, J. T. Aberle, B. Bakkaloglu, and C. Chakrabarti, "Automatic antenna tuning unit for software-defined and cognitive radio," in *Proc. IEEE Antennas Propag. Soc. Int. Symp.*, Honolulu, HI, USA, Jun. 2007, pp. 85–88.

[8] X. Zhao, S. Riaz, and S. Geng, "A reconfigurable MIMO/UWB MIMO antenna for cognitive radio applications," *IEEE Access*, vol. 7, pp. 46739–46747, 2019.

[9] Z. Wu, H. Liu, and L. Li, "Metasurface-inspired low profile polarization reconfigurable antenna with simple DC controlling circuit," *IEEE Access*, vol. 7, pp. 45073–45079, 2019.

[10] D. E. Anagnostou, Z. Guizhen, M. T. Chryssomallis, J. C. Lyke, G. E. Ponchak, J. Papapolymerou, and C. G. Christodoulou, "Design, fabircation, and measurements of an RF-MEMS-based self-similar reconfigurable antenna," *IEEE Trans. Antennas Propag.*, vol. 54, no. 2, pp. 422–432, Feb. 2006.

[11] A. Grau Besoli and F. De Flaviis, "A multifunctional reconfigurable pixeled antenna using MEMS technology on printed circuit board," *IEEE Trans. Antennas Propag.*, vol. 59, no. 12, pp. 4413–4424, Dec. 2011.

[12] M. D. Wright, W. Baron, J. Miller, J. Tuss, D. Zeppettella, and M. Ali, "MEMS reconfigurable broadband patch antenna for conformal applications," *IEEE Trans. Antennas Propag.*, vol. 66, no. 6, pp. 2770–2778, Jun. 2018.

[13] A. Pourghorban Saghati, J. Singh Batra, J. Kameoka, and K. Entesari, "Miniature and reconfigurable CPW folded slot antennas employing liquid-metal capacitive loading," *IEEE Trans. Antennas Propag.*, vol. 63, no. 9, pp. 3798–3807, Sep. 2015.

[14] Y. Tawk, J. Costantine, K. Avery, and C. G. Christodoulou, "Implementation of a cognitive radio front-end using rotatable controlled reconfigurable antennas," *IEEE Trans. Antennas Propag.*, vol. 59, no. 5, pp. 1773–1778, May 2011.

[15] C. Wu, T. Wang, A. Ren, and D. G. Michelson, "Implementation of reconfigurable patch antennas using reed switches," *IEEE Antennas Wireless Propag. Lett.*, vol. 10, pp. 1023–1026, 2011.

[16] Q. Liu, N. Wang, Q. Zeng, C. Wu, and G. Wei, "A frequency reconfigurable patch antenna with reed switches," presented at the IEEE Int. Wireless Symp. (IWS), X 'ian China, Mar. 2014.

[17] C. Wu, Y. Zhang, and Q. Liu, "A magnetically controlled reconfigurable antenna using a reed switch," presented at the IEEE Int. Conf. Signal Process., Commun. Comput. (ICSPCC), KunMing, China, Aug. 2013.

[18] Y. Tawk, J. Costantine, S. Hemmady, G. Balakrishnan, K. Avery, and C. G. Christodoulou, "Demonstration of a cognitive radio front end using an optically pumped reconfigurable antenna system (OPRAS)," *IEEE Trans. Antennas Propag.*, vol. 60, no. 2, pp. 1075–1083, Feb. 2012.

[19] D. Rodrigo, L. Jofre, and B. A. Cetiner, "Circular beam-steering reconfigurable antenna with liquid metal parasitics," *IEEE Trans. Antennas Propag.*, vol. 60, no. 4, pp. 1796–1802, Apr. 2012.

[20] A. Iftikhar, J. Allen, B. D. Braaten, M. Allen, S. Asif, and J. Parrow, "Improving the efficiency of a reconfigurable microstrip patch using magneto-static field responsive structures," *Electron. Lett.*, vol. 52, no. 14, pp. 1194–1196, Jul. 2016.

[21] M. U. Khan, M. S. Sharawi, and R. Mittra, "Microstrip patch antenna miniaturization techniques: A review," *IET Microw., Ant. Propag.*, vol. 9, no. 9, pp. 913–922, 2015.

[22] Y. Dong and T. Itoh, "Metamaterial-based antennas," *Proc. IEEE*, vol. 100, no. 7, pp. 2271–2285, Jul. 2012.

[23] (2015). *Reed Switch—KSK-1A04*. Meder Electronic, Singen, Germany. [Online]. Available: www.standexmeder.com

[24] J. Parrow, "Equivalent circuit modeling and signal integrity analysis of magneto-static responsive structures, and their applications in changing the effective permittivity of microstrip transmission lines," Ph.D. dissertation, Elec. Comp. Engg. Dept., North Dakota State Univ., Fargo, North Dakota, 2016.

[25] *Potters Industries LLC*. Accessed: Dec. 15, 2015. [Online]. Available: http://www.pottersbeads.com/

[26] *Rogers Corporation*. Accessed: Sep. 15, 2017. [Online]. Available: www.rogerscorp.com

[27] W.-Y. Hsiang, "On the sphere packing problem and the proof of Kepler's problem conjecture," *Int. J. Math.*, vol. 4, no. 5, pp. 739–831, Oct. 1993.

[28] *ANSYS High Frequency Simulation Software (HFSS)*. Accessed: Sep. 15, 2017. [Online]. Available: www.ansys.com

[29] A. Grau, J. Romeu, M.-J. Lee, S. Blanch, L. Jofre, and F. De Flaviis, "A Dual-Linearly-Polarized MEMS-reconfigurable antenna for narrowband MIMO communication systems," *IEEE Trans. Antennas Propag.*, vol. 58, no. 1, pp. 4–17, Jan. 2010.

[30] S. Nikolaou, R. Bairavasubramanian, C. Lugo, I. Carrasquillo, D. C. Thompson, G. E. Ponchak, J. Papapolymerou, and M. M. Tentzeris, "Pattern and frequency reconfigurable annular slot antenna using PIN diodes," *IEEE Trans. Antennas Propag.*, vol. 54, no. 2, pp. 439–448, Feb. 2006.

[31] M. Shirazi, T. Li, and X. Gong, "Effects of PIN diode switches on the performance of reconfigurable slot-ring antenna," in *Proc. IEEE 16th Annu. Wireless Microw. Technol. Conf. (WAMICON)*, Apr. 2015, pp. 1–3.

[32] Q. Liu, N. Wang, C. Wu, G. Wei, and A. B. Smolders, "Frequency reconfigurable antenna controlled by multi-reed switches," *IEEE Antennas Wireless Propag. Lett.*, vol. 14, pp. 927–930, 2015.

ADNAN IFTIKHAR (Member, IEEE) received the B.S. degree in electrical engineering from COMSATS University Islamabad (CUI), Pakistan, the M.S. degree in personal mobile and satellite communication from the University of Bradford, U.K., and the Ph.D. degree in electrical and computer engineering from North Dakota State University (NDSU), USA, in 2008, 2010, and 2016, respectively.

He is currently an Assistant Professor with the Department of Electrical and Computer Engineering, COMSATS University Islamabad (CUI). He has authored or coauthored 50 journals and conference publications. His current research interests include applied electromagnetic, reconfigurable antennas, leaky wave antennas, phased array antennas, and energy harvesting for low power devices.

SAJID MEHMOOD ASIF (Member, IEEE) received the M.S. degree in radio frequency communication engineering from the University of Bradford, U.K., in 2006, and the Ph.D. degree in electrical and computer engineering from North Dakota State University (NDSU), Fargo, ND, USA, in 2017.

He is currently a Research Associate in frequency agile radio with The University of Sheffield, U.K. He has authored or coauthored more than 60 peer-reviewed journal and conference papers. His research interests include RF/microwave circuits, printed antennas, implantable antennas, wireless sensors, and energy harvesting for biomedical applications. He is a member of Tau Beta Pi and the IEEE-Eta Kappa Nu. He has received numerous awards and scholarships, including the internationally prestigious IEEE-AP-S Doctoral Research Grant, in 2015, the NSF funded ND-EPSCOR Doctoral Dissertation Assistantship Award, from 2005 to 2016, and First-Place in the NDSU Innovation Challenge Competition, in 2017. He served the IEEE Red River Valley Section as the Chair, in 2015, and the Vice-Chair, in 2014.

JACOB M. PARROW received the B.S. degree in electrical engineering and the M.S. degree in electrical engineering with a focus in electromagnetics from North Dakota State University, Fargo, ND, USA, in 2015 and 2016, respectively.

He is currently working full time with the Department of Defense Contractor to develop his skills within his fields of interest, which include antenna's, electromagnetics, RF/microwave circuits, and signal integrity.

Mr. Parrow is a General Class Ham Radio Operator (KD0PXY) who enjoys the hobby when time allows.

JEFFERY W. ALLEN (Senior Member, IEEE) received the Ph.D. degree in electrical engineering from Duke University, Durham, NC, USA, in 2011.

He is a Senior Research Electronics Engineer with the Air Force Research Laboratory, Munitions Directorate, Eglin Air Force Base, FL, USA. He spent several years in the industry working on passive optical networking components, vertical cavity surface emitting lasers, RF and radar systems, and RF systems for code division multiple access cellphone base stations. He has previously worked in the Air Force Research Laboratory, Sensors Directorate at Hanscom AFB and Wright Paterson AFB. His primary research interests focus on electromagnetic wave matter interaction and research in novel sensing paradigms. His current research interests include development of analytical models, computational electromagnetics, and fabrication techniques for engineered electromagnetic structures and applying them to systems in a wide area of applications. His research interests include the areas of metamaterials, optimized RF apertures, conformal/structurally integrated apertures, semiconductor physics, IR plasmonics, nonlinear optics, quantum sensing, and nanofabrication.

Dr. Allen is affiliated with the electrical engineering honor society, Eta Kappa Nu; engineering honor society, Tau Beta Pi; honor society of science and engineering research, Sigma Xi; and the professional organization, IEEE.

MONICA S. ALLEN (Senior Member, IEEE) received the Ph.D. degree in electrical engineering from the University of Texas at Arlington, Arlington, TX, USA, in 2006.

She is currently a Senior Research Electronics Engineer with the Air Force Research Laboratory, Munitions Directorate, Eglin Air Force Base, FL, USA. Her current projects range from modeling, simulation, and fabrication of micro- and nanostructures for gain and selectivity enhancement to characterization of fabricated devices to test their performance. She spent several years in the industry working on highly sensitive sensing systems based on optical arrays and magnetostrictive materials. In the past, she has worked at the Air Force Research Laboratory, Sensors Directorate at Hanscom AFB and Wright Paterson AFB. Her research focuses on resonant sensing platforms for EO/IR technologies and components that can find applications in detection and sensing. Her primary research interests include nonlinear optical, photonic, and plasmonic physics concepts through the exploitation of light–matter interactions. Her other research interests include investigation of nonlinear optical phenomena and quantum photonic devices at infrared wavelengths.

Dr. Allen is affiliated with the electrical engineering honor society, Eta Kappa Nu; engineering honor society, Tau Beta Pi; honor society of science and engineering research, Sigma Xi; and the professional organization, IEEE.

ADNAN FIDA received the M.S. degree in broadband mobile communication from Lancaster University, U.K., and the Ph.D. degree from Universiti Brunei Darusallam, Brunei. in 2010 and 2015, respectively. He is currently working as an Assistant Professor with the Department of Electrical Engineering, COMSATS Institute of Information Technology, Islamabad, Pakistan. He has a knack for working on diversified projects related to RF and wireless sensor networks, such as the development of algorithms for optimizing of the information link capacity and route optimization in mobile sensor networks. A simulator is built for implementation and validation of the proposed algorithms. He is currently focusing on the energy harvesting from ambient sources to power the sensor nodes with low power requirements.

BENJAMIN D. BRAATEN (Senior Member, IEEE) received the B.S. degree in electrical engineering, the M.S. degree in electrical engineering, and the Ph.D. degree in electrical and computer engineering from North Dakota State University, Fargo, ND, USA, in 2002, 2005, and 2009, respectively.

In 2009 Fall semester, he held a postdoctoral research position at the South Dakota School of Mines and Technology, Rapid City, SD, USA. At the end of the 2009 Fall semester, he joined the Electrical and Computer Engineering Department, North Dakota State University, and was promoted to Associate Professor with tenure, in 2015. He is currently the Chairman of the ECE Department, NDSU. He has authored or coauthored more than 100 peer-reviewed journal and conference publications, several book chapters on the design of antennas for radio frequency identification, and holds one U.S. patent on wireless pacing of the human heart. His research interests include printed antennas, conformal self-adapting antennas, microwave devices, topics in EMC, topics in BIOEM, and methods in computational electromagnetics.

Dr. Braaten received the College of Engineering and Architecture Graduate Researcher of the Year and the College of Engineering and Architecture Graduate Teacher of the Year awards. He also serves as an Associate Editor for the IEEE Antennas and Wireless Propagation Letters and is a member of the National Honorary Mathematical Society PI MU EPSILON.